Supporting Information for "Dust storm-enhanced gravity wave activity in the Martian thermosphere observed by MAVEN and implications for atmospheric escape"

Erdal Yiğit[1], Alexander S. Medvedev[2], Mehdi Benna[3,4], Bruce Jakosky[5]

[1]George Mason University, Department of Physics and Astronomy.
[2]Max Planck Institute for Solar System Research, Gø"ttingen, Germany.
[3]University of Maryland Baltimore County, Baltimore, MD, USA.
[4]Solar System Exploration Division, NASA Goddard Space Flight Center, Greenbelt, MD, USA.
[5]Laboratory for Atmospheric and Space Physics, University of Colorado, CO, USA.

Contents of this file

1 Text for Figures S1 to S4

1.1 Neutral Gas and Ion Mass Spectrometer Instrument onboard MAVEN

NASA's Mars Atmosphere and Volatile Evolution Mission (MAVEN) spacecraft orbits Mars since 21 September 2014. Its prime mission is to study the Martian upper atmosphere. It has an orbital period of about 4.5 hours, an inclination of $75°$, and a nominal periapsis of 150-160 km. Our GW analysis utilizes data from the NGIMS instrument, which is a quadrupole mass spectrometer with a mass range of 2-150 Da and a unit mass resolution. It was designed to fully characterize the composition and abundances of neutrals and ions in the Martian upper atmosphere. NGIMS collects its measurements every orbit when the altitude of the MAVEN spacecraft descends below 500 km. During that segment of the orbit, the instrument's narrow field of view is maintained by the spacecraft's Actuated Payload Platform (APP) within $2°$ of the spacecraft ram direction to maximize the measured signal. Since the pointing stability of the APP is better than $0.2°$, most of the measured signal fluctuations reflect variations of neutral densities along the spacecraft track. Detailed description of the data processing procedures of the NGIMS neutral gas measurements is provided in (Benna & Elrod, 2015). The standard deviation of individual measurements due to random uncertainties is dependent on the density level and is typically $\sim 10\%$ at 7×10^5 cm^{-3}, and $< 1\%$ above 5×10^5 cm^{-3}. The instrumental background level is species-dependent and is typically ~ 105 cm^{-3} for carbon dioxide.

1.2 Data Coverage in MY 34

For the analysis of the GW activity before and during the planet-encircling global dust storm (GDS), we consider data from NGIMS onboard the MAVEN spacecraft from 1 May 2018 till 30 September 2018, corresponding to $L_s = 167° - 259.6°$ in Martian Year (MY) 34.

We use NGIMS Level 2 data, version 8, which are publicly available at the Planetary Data System (PDS). In total 683 NGIMS orbits (profiles) are used for the GW activity analysis in MY 34 (2018). Coverage of the data for the different periods are seen in Supplementary Figure S1. Each orbit is composed of an inbound and an outbound pass, which are both included in our analysis from 240 km to 160 km, which is close to the nominal periapsis altitude, (panel a). With an orbital period of ~ 4.5h, MAVEN delivers up to five data profiles (inbound and outbound pass) per day. During the deep dip campaigns the spacecraft periapsis is as low as ~ 140 km. In order to assess the variations of GW activity, we have divided the observations into ten approximately 15-day (~ 15-sol) intervals, each containing about 60-79 orbits, where the corresponding periods are shown with different colors in Supplementary Figure S1. It takes about 700 seconds for the spacecraft to cover an altitude range between 140 and 240 km (Figure S1a). MAVEN has a very good longitudinal coverage during all chosen periods (Figure S1b). It is seen that the latitude coverage moves overall from southern midlatitudes to northern high-latitudes and the local time coverage changes during the period of analysis. Specifically, latitudes from $60°$S–$70°$N and local times from 0 to 12 h and 15 to 24 h are covered during the analyzed MY 34 period (Figures S1c-d). Carbon dioxide density profiles as a function of the inbound and outbound passes from all used orbits are seen next (Figure S1e). Maximum number densities are around the periapsis and are in the order of 10^9 cm^{-3}. Good longitude coverage and limited latitude coverage for the time intervals are seen in Figure S1f.

1.3 Intercomparison of MY 33 and MY 34: Data coverage

For the comparison of the dust-storm GW activity in MY 34 with a low-dust period, presented in Figure 2, NGIMS data with similar seasonal and spatiotemporal coverage are chosen one Martian year earlier. That is, the low-dust period in MY 33 with solar longitudes $L_s = 171.7° - 191.6°$ (20 June-25 July 2016) is compared with the representative dust storm period in MY 34, $L_s = 202.8° - 224.2°$ (1 July-5 August 2018), MAVEN has comparable latitude and local time coverages presented in Figure S2. In both periods, the spacecraft needs about 500-550 s to cover the altitude range between 160 and 200 km (panel a), it samples a common latitude sector between $15°$S-$45°$ N (panel b) and a common local time sector between about 1.5 h- 4.5 h. These relative orbital coverages are also seen in Figure 2.

1.4 Example of GW analysis

To illustrate the quantification of the GW-induced density fluctuation, we choose a representative orbit on 31 May 2018 (MY 34, $L_s = 184.6°$), just before the onset of the GDS, presented in Figure S3. The inbound and outbound motion from 240 km to 160 km takes about 600 s (a) and covers $\pm 6°$ in longitude (b), 50S-10S in latitude (c), and 9 h in local time (d). The associated quantification of the GW activity is shown in Figure S4. The original carbon dioxide density during the inbound and outbound pass in red is shown in a logarithmic scale in (a) and in a linear scale in (b). The 7th-order polynomial fit to the logarithm of the density is shown in blue in (a). The difference between the instantaneous density and the mean yields the fluctuation component, which upon normalization with respect to the mean yields the wave-induced relative density fluctuation, as shown in panel (c) in percentage. The fluctuations are up to $\pm 40\%$. The values in the initial and end phases of the orbit are representative of high-altitude values of GWs, as can be seen from Figure S3a and S4c. In evaluation of the mean GW activity, the absolute values of the density fluctuations, $|\rho'|$, are considered. Then, $|\rho'|$ data points within each bin are used to determine the mean value for that bin.

References

Benna, M., & Elrod, M. (2015). *NGIMS PDS Software Interface Specification, (MAVEN-NGIMS-SIS-0001), PDS Atmospheres Node,*. Retrieved from `http://atmos.pds.nasa.gov/data_and_services/atmospheres_data/MAVEN/ngims.html`
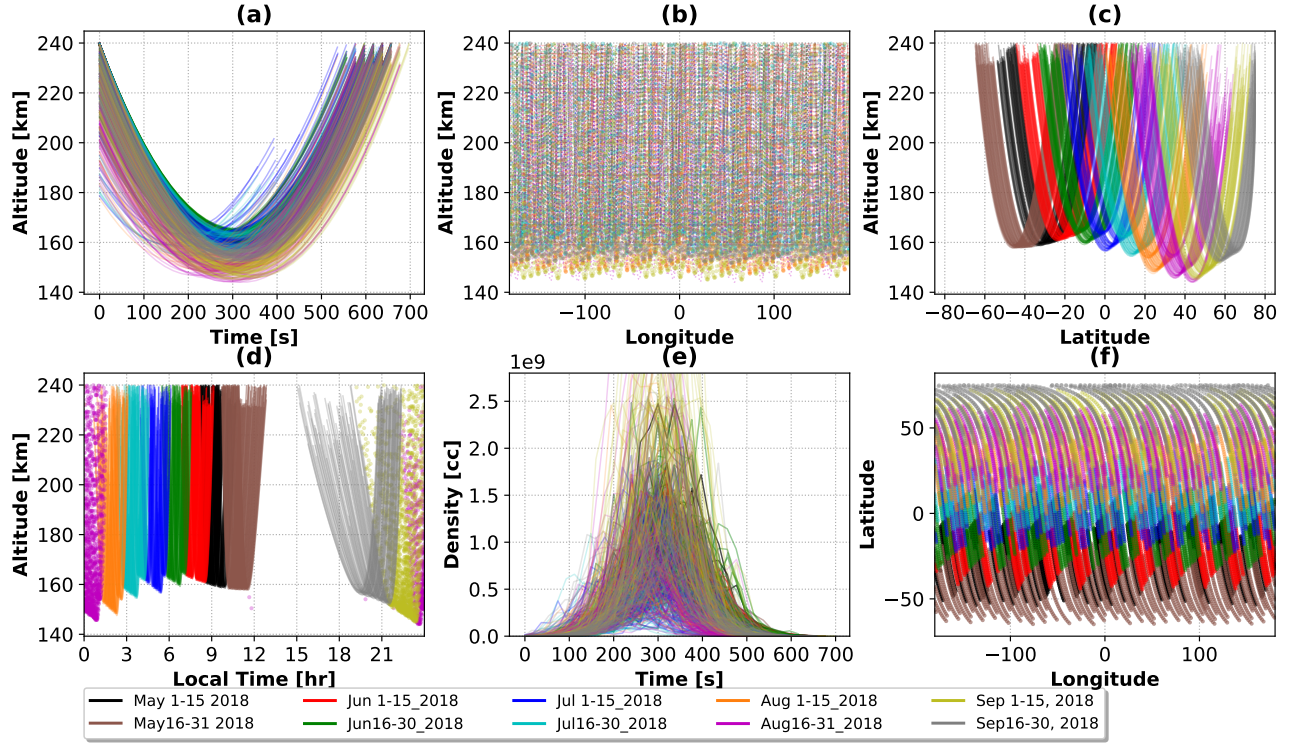
2 Figures S1 to S4

Figure S1. NGIMS/MAVEN data coverage from 1 May 2018 till 30 September 2018, corresponding to $L_s = 167° - 259.6°$ in Martian Year (MY) 34. In total 683 passes have been included (inbound and outbound), organized approximately by 15-day (~15-sol) intervals, represented by different colors. The coverage is presented in terms of (a) altitude-time, (b) altitude-longitude, (c) altitude-latitude, (d) altitude-local time, (e) carbon dioxide density-time, and (f) latitude-longitude. Data points between 140 and 240 km have been included in the analysis.
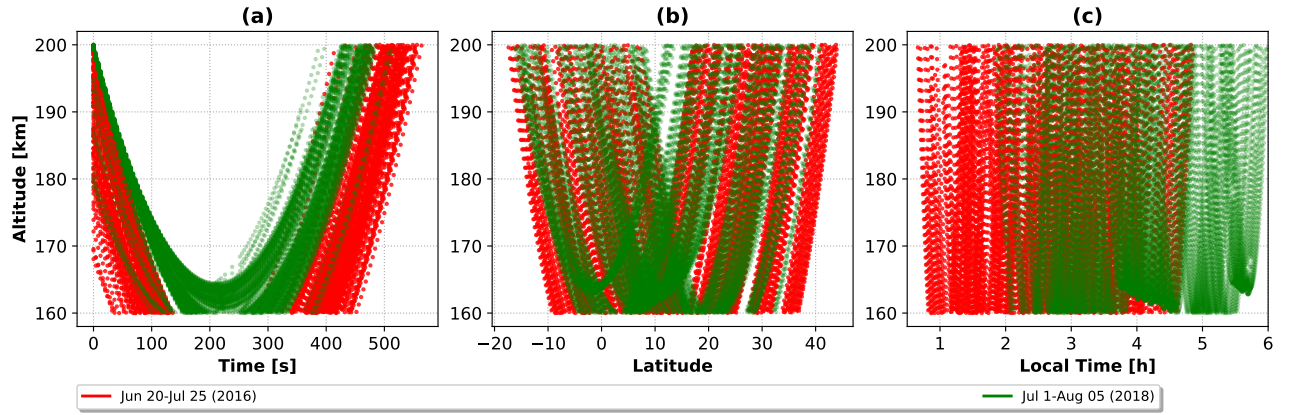
Figure S2. NGIMS/MAVEN data used for intercomparison of a low-dust period in MY 33 (20 June-25 July 2016, $L_s = 171.7° - 191.6°$, red) and dust-storm period in MY 34 (1 July-6 August 2018, $L_s = 202.8° - 224.2°$, green). In total 327 passes (inbound and outbound) are included in this analysis with 164 and 163 orbits in the chosen MY 33 and MY 34 periods, respectively. The coverage is presented in terms of (a) altitude-time, (b) altitude-latitude, and (c) altitude-local time variations. Data points between 160 and 200 km have been included for the analysis.
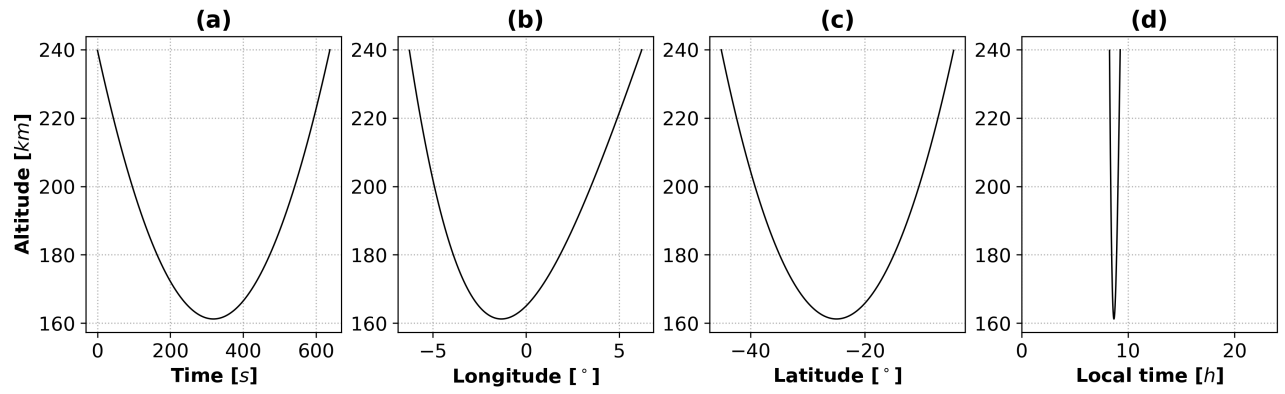
Figure S3. Spatial and temporal coverage for a representative orbit on 31 May 2018 (MY 34, $L_s = 184.6°$) before the onset of the GDS. Altitude variations of the orbit as a function of (a) time, (b) longitude, (c) latitude, and (d) local time variations are demonstrated.
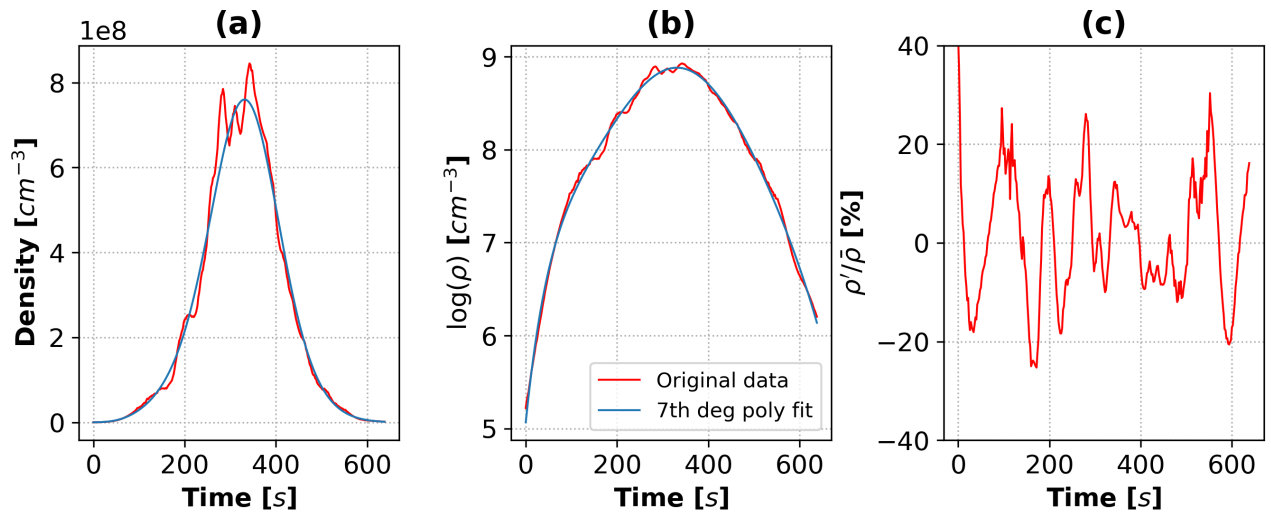
Figure S4. Quantification of gravity wave-induced density fluctuations for the representative orbit shown in Fig S3. (a) Instantaneous carbon dioxide density fluctuations (red), including inbound and outbound passes, and the background mean density (blue) determined by fitting a 7th order polynomial fit to the instantaneous density variations. (b) Same as (a) but in logarithmic scale; (c) the relative density fluctuation in percentage.